



Product Manual

# OxiSelect™ Protein Carbonyl Immunoblot Kit

Catalog Number

STA-308

10 blots

**FOR RESEARCH USE ONLY**  
Not for use in diagnostic procedures

---

**Gentaur Molecular Products BVBA**

**Address:** Voortstraat 49, 1910 Kampenhout, Belgium

**T:** 0032 16 58 90 45 | **E:** [info@gentaur.com](mailto:info@gentaur.com)

**Websites:** [www.gentaur.com](http://www.gentaur.com) | [www.maxanim.com](http://www.maxanim.com)

## **Introduction**

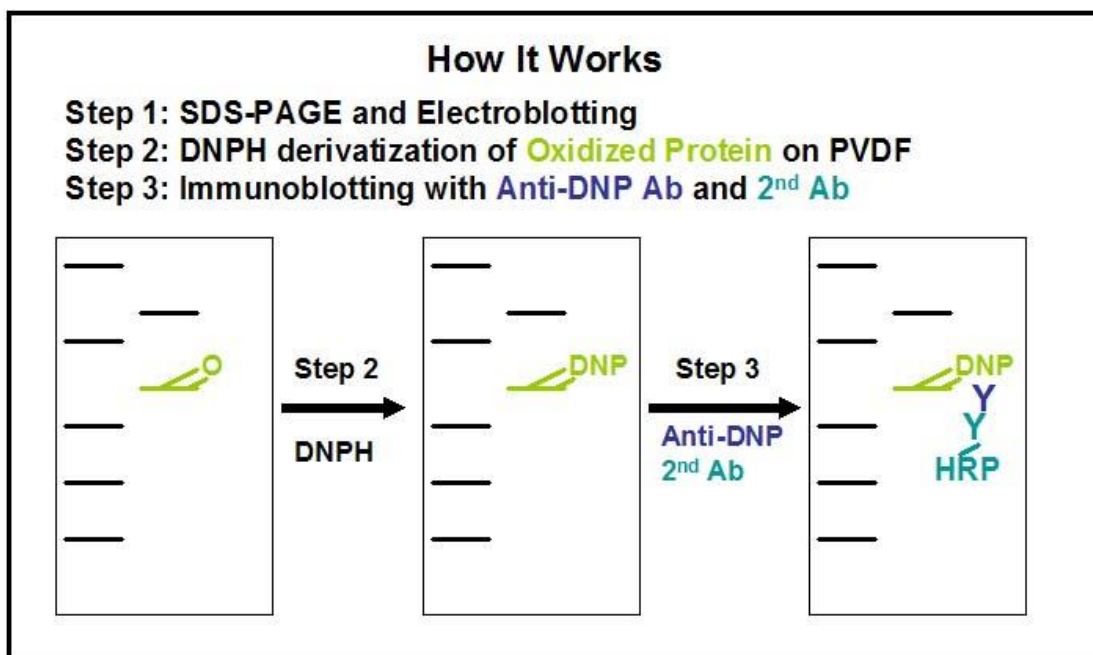
Protein oxidation is defined as the covalent modification of a protein induced either directly by reactive oxygen species or indirectly by reaction with secondary by-products of oxidative stress. Oxidative modification of proteins can be induced *in vitro* by a wide array of pro-oxidant agents and occurs *in vivo* during aging and in certain disease conditions.

There are numerous types of protein oxidative modification. The most common products of protein oxidation in biological samples are the protein carbonyl derivatives of Pro, Arg, Lys, and Thr. These derivatives are chemically stable and serve as markers of oxidative stress for most types of ROS.

Many of the current assays involve pre-derivatization of the carbonyl group with dinitrophenylhydrazine (DNPH) prior to electrophoresis, followed by immunoblotting with an anti-DNP antibody. Unfortunately, this pre-derivatization alters the electrophoretic (and electrofocusing) properties of proteins. Consequently, it is not possible to directly compare the patterns from "oxidized" fingerprints with those from "non-oxidized" protein fingerprints. Cell Biolabs' Protein Carbonyl Immunoblot Kit has the ability to conduct all derivatization and staining **after** electrophoresis and transblotting. This allows one to directly compare oxidized vs. non-oxidized protein fingerprints.

The OxiSelect™ Protein Carbonyl Immunoblot Kit offers a simple and complete system for the detection of protein oxidation. This kit also includes a Protein Oxidation Immunoblot Control as positive control. Each kit provides sufficient quantities to perform at least 10 blots (7.5 cm X 8.5 cm).

## **Assay Principle**



## **Related Products**

1. STA-305: OxiSelect™ Nitrotyrosine ELISA Kit
2. STA-309: Oxidized Protein Immunoblot Control (Carbonyl-BSA)
3. STA-310: OxiSelect™ Protein Carbonyl ELISA Kit
4. STA-318: OxiSelect™ AOPP Assay Kit
5. STA-817: OxiSelect™ Advanced Glycation End Products (AGE) Competitive ELISA

## **Kit Components**

1. Rabbit Anti-DNP Antibody (Part No. 230801): One 100 µL tube
2. Secondary Antibody, HRP-conjugate (Part No. 230805): One 100 µL tube
3. Protein Oxidation Immunoblot Control (Part No. 230803): One 100 µL tube (provided ready-to-use oxidized BSA in 1X reducing SDS-PAGE Sample Buffer, pre-boiled)
4. 10X DNPH Solution (Part No. 230804): One 20 mL amber bottle

## **Materials Not Supplied**

1. Protein MW standards
2. Reducing SDS-PAGE Sample Buffer
3. Polyacrylamide gels such as precast gels available from Invitrogen or BioRad
4. Electrophoresis Buffers
5. Electrophoresis and Western Blot Transfer Systems
6. Immunoblotting Buffers such as TBST (20 mM Tris-HCl, pH 7.4, 0.15 M NaCl, 0.05% Tween-20)
7. PVDF or Nitrocellulose Membrane (PVDF is recommended)
8. Methanol
9. 2N HCl
10. Non-fat Dry Milk
11. ECL Reagents

## **Storage**

Upon receipt, store the 10X DNPH Solution at 4°C. Aliquot and store all other components at -20°C to avoid multiple freeze/thaw cycles.

## **Assay Protocol**

### **I. Electrophoresis and Transblotting**

1. Prepare samples for electrophoresis with reducing SDS Sample Buffer.
2. Load 20 µL of Protein Oxidation Immunoblot Control (provided ready-to-use, pre-boiled) or sample to wells of a polyacrylamide gel. Also, it's recommended to include a pre-stained MW

standard (as indicator of a successful transfer in step 3). Run the gel as per the manufacturer's instructions.

3. Transfer the gel proteins to a PVDF membrane as per the manufacturer's instructions.

*Note: We recommend using PVDF membrane instead of Nitrocellulose due to its low background signal after derivatization, resulting in stronger chemiluminescent signal.*

## **II. Derivatization (all steps are at room temperature, with shaking)**

1. Following the electroblotting step, immerse the PVDF membrane in 100% Methanol for 15 seconds, and then allow it to dry at room temperature for 5 minutes.

*Note: If Nitrocellulose is used instead of PVDF, this step should be skipped.*

2. Equilibrate the membrane in TBS containing 20% Methanol for 5 minutes.
3. Wash the membrane in 2N HCl for 5 minutes.
4. Prepare sufficient amount of 1X DNPH solution by diluting the 10X DNPH Solution in 2N HCl. Incubate the membrane with 1X DNPH solution for exactly 5 minutes.

*Note: 1X DNPH Solution is stable for one week when stored in the dark at 4°C. Do not freeze.*

5. Wash the membrane three times in 2N HCl, 5 minutes each time.
6. Next, wash the membrane five times in 100% methanol (PVDF) or 50% methanol (Nitrocellulose), 5 minutes each time.

## **III. Immunoblotting**

1. Block the DNPH-treated membrane with 5% non-fat dry milk in TBST for 1 hr at room temperature with constant agitation.
2. Wash the blocked membrane three times with TBST, 5 minutes each time.
3. Incubate the membrane with Rabbit Anti-DNP Antibody, freshly diluted 1:1000 in 5% non-fat dry milk/TBST, for 1-2 hr at room temperature with constant agitation.
4. Wash the blotted membrane three times with TBST, 5 minutes each time.
5. Incubate the membrane with Secondary Antibody, HRP-conjugate, freshly diluted 1:1000 in 5% non-fat dry milk/TBST, for 1 hr at room temperature with constant agitation.
6. Wash the blotted membrane five times with TBST, 5 minutes each time.
7. Use the detection method of your choice. We recommend enhanced chemiluminescence reagents from Pierce.

## **Example of Results**

The following figure demonstrates typical blot results of oxidized BSA after DNPH derivation. One should use the data below for reference only. This data should not be used to interpret actual results.



**Figure 1: Immunoblotting of Oxidized BSA.** Carbonyl-BSA, Oxidation Immunoblot Control, was first electroblotted onto nitrocellulose membrane. Following the electroblotting procedure, the membrane was incubated with (right strip) or without (left strip) DNPH solution. The derivatized Carbonyl-BSA is detected by immunoblotting with anti-DNP antibody as described in the Assay Protocol.

## References

1. Cadenas, E., Boveris, A., Ragan, CI., and Stoppani, AO. (1977). *Archives of Biochemistry & Biophysics* **180**:248–257.
2. Wakeyama, H., Takeshige, K., Takayanagi, R., and Minakami, S. (1982). *Biochem J.* **205**:593–601.
3. Talent, JM., Kong, Y., and Gracy, RW. (1998). *Anal. Biochem.* **263**:31–38.

## Recent Product Citations

1. Ngwaga, T. et al. (2023). Effector-mediated subversion of proteasome activator (PA)28 $\alpha\beta$  enhances host defense against *Legionella pneumophila* under inflammatory and oxidative stress conditions. *PLoS Pathog.* **19**(6):e1011473. doi: 10.1371/journal.ppat.1011473.
2. Capó, X. et al. (2023). Hyperbaric Oxygen Therapy Reduces Oxidative Stress and Inflammation, and Increases Growth Factors Favouring the Healing Process of Diabetic Wounds. *Int J Mol Sci.* **24**(8):7040. doi: 10.3390/ijms24087040.
3. Yamashima, T. et al. (2023). Vegetable Oil-Peroxidation Product 'Hydroxynonenal' Causes Hepatocyte Injury and Steatosis via Hsp70.1 and BHMT Disorders in the Monkey Liver. *Nutrients.* **15**(8):1904. doi: 10.3390/nu15081904.
4. Pollock, N. et al. (2023). Deletion of Sod1 in Motor Neurons Exacerbates Age-Related Changes in Axons and Neuromuscular Junctions in Mice. *eNeuro.* **10**(3): ENEURO.0086-22.2023. doi: 10.1523/ENEURO.0086-22.2023.

5. Tsuzuki, T. et al. (2022). Exercise training improves obesity-induced inflammatory signaling in rat brown adipose tissue. *Biochem Biophys Res Commun.* doi: 10.1016/j.bbrep.2022.101398.
6. Zhou, Z.D. et al. (2022). The role of tyrosine hydroxylase-dopamine pathway in Parkinson's disease pathogenesis. *Cell Mol Life Sci.* **79**(12):599. doi: 10.1007/s00018-022-04574-x.
7. Musci, R.V. et al. (2022). Phytochemical compound PB125 attenuates skeletal muscle mitochondrial dysfunction and impaired proteostasis in a model of musculoskeletal decline. *J Physiol.* doi: 10.1113/JP282273.
8. Monserrat-Mesquida, M. et al. (2022). A Greater Improvement of Intrahepatic Fat Contents after 6 Months of Lifestyle Intervention Is Related to a Better Oxidative Stress and Inflammatory Status in Non-Alcoholic Fatty Liver Disease. *Antioxidants (Basel).* **11**(7):1266. doi: 10.3390/antiox11071266.
9. Yoshihara, T. et al. (2022). Losartan treatment attenuates hindlimb unloading-induced atrophy in the soleus muscle of female rats via canonical TGF- $\beta$  signaling. *J Physiol Sci.* **72**(1):6. doi: 10.1186/s12576-022-00830-8.
10. Packialakshmi, B. et al. (2022). Tourniquet-induced lower limb ischemia/reperfusion reduces mitochondrial function by decreasing mitochondrial biogenesis in acute kidney injury in mice. *Physiol Rep.* **10**(3): e15181. doi: 10.14814/phy2.15181.
11. Tian, L. et al. (2022). Microtubule Affinity-Regulating Kinase 4 Promotes Oxidative Stress and Mitochondrial Dysfunction by Activating NF- $\kappa$ B and Inhibiting AMPK Pathways in Porcine Placental Trophoblasts. *Biomedicines.* **10**(1):165. doi: 10.3390/biomedicines10010165.
12. Daussin, F.N. et al. (2021). Dietary Cocoa Flavanols Enhance Mitochondrial Function in Skeletal Muscle and Modify Whole-Body Metabolism in Healthy Mice. *Nutrients.* **13**(10):3466. doi: 10.3390/nu13103466.
13. Hahn, D. et al. (2021). Nox4 Knockout Does Not Prevent Diaphragm Atrophy, Contractile Dysfunction, or Mitochondrial Maladaptation in the Early Phase Post-Myocardial Infarction in Mice. *Cell Physiol Biochem.* **55**(4):489-504. doi: 10.33594/000000400.
14. Jeong, J. et al. (2021). The butyrophilin 1a1 knockout mouse revisited: Ablation of Btn1a1 leads to concurrent cell death and renewal in the mammary epithelium during lactation. *FASEB Bioadv.* doi: 10.1096/fba.2021-00059.
15. Oliva Chávez, A.S. et al. (2021). Tick extracellular vesicles enable arthropod feeding and promote distinct outcomes of bacterial infection. *Nat Commun.* **12**(1):3696. doi: 10.1038/s41467-021-23900-8.
16. Monserrat-Mesquida, M. et al. (2020). Oxidative Stress and Pro-Inflammatory Status in Patients with Non-Alcoholic Fatty Liver Disease. *Antioxidants (Basel).* **9**(8): E759. doi: 10.3390/antiox9080759.
17. Yagisawa, Y. et al. (2020). Effects of occlusal disharmony on cardiac fibrosis, myocyte apoptosis and myocyte oxidative DNA damage in mice. *PLoS One.* **15**(7): e0236547. doi: 10.1371/journal.pone.0236547.
18. Song, W. et al. (2020). Baicalin combats glutamate excitotoxicity via protecting glutamine synthetase from ROS-induced 20S proteasomal degradation. *Redox Biol.* doi: 10.1016/j.redox.2020.101559.
19. Capó, X. et al. (2020). Calorie Restriction Improves Physical Performance and Modulates the Antioxidant and Inflammatory Responses to Acute Exercise. *Nutrients.* **12**:930. doi: 10.3390/nu12040930.
20. Pons, D.G. et al. (2020). Micronutrients Selenomethionine and Selenocysteine Modulate the Redox Status of MCF-7 Breast Cancer Cells. *Nutrients.* **12**(3). pii: E865. doi: 10.3390/nu12030865.

21. Tian, L. et al. (2020). Impaired Mitochondrial Function Results from Oxidative Stress in the Full-Term Placenta of Sows with Excessive Back-Fat. *Animals (Basel)*. **10**(2). pii: E360. doi: 10.3390/ani10020360.
22. Geicu, O.I. et al. (2020). Dietary AGEs involvement in colonic inflammation and cancer: insights from an in vitro enterocyte model. *Sci Rep*. **10**(1):2754. doi: 10.1038/s41598-020-59623-x.
23. Yin, B. et al. (2019). PtomtAPX, a mitochondrial ascorbate peroxidase, plays an important role in maintaining the redox balance of *Populus tomentosa* Carr. *Sci Rep*. **9**(1):19541. doi: 10.1038/s41598-019-56148-w.
24. Adeluyi, A. et al. (2019). Microglia morphology and proinflammatory signaling in the nucleus accumbens during nicotine withdrawal. *Sci Adv*. **5**(10): eaax7031. doi: 10.1126/sciadv. aax7031.
25. Koike, S. et al. (2019). Age-related alteration in the distribution of methylglyoxal and its metabolic enzymes in the mouse brain. *Brain Res Bull*. **144**:164-170. doi: 10.1016/j.brainresbull.2018.11.025.
26. Park, A.M. et al. (2018). Heat shock protein 27 promotes cell cycle progression by down-regulating E2F transcription factor 4 and retinoblastoma family protein p130. *J Biol Chem*. **293**(41):15815-15826. doi: 10.1074/jbc.RA118.003310.
27. Hernández-López, R. et al. (2018). Non-tumor adjacent tissue of advanced stage from CRC shows activated antioxidant response. *Free Radic Biol Med*. **126**:249-258. doi: 10.1016/j.freeradbiomed.2018.08.021.
28. Harmon, D.B. et al. (2018). Adipose tissue-derived free fatty acids initiate myeloid cell accumulation in mouse liver in states of lipid oversupply. *Am J Physiol Endocrinol Metab*. **315**(5): E758-E770. doi: 10.1152/ajpendo.00172.2018.
29. Wei, Y. et al. (2018). Oxidation of KCNB1 channels in the human brain and in mouse model of Alzheimer's disease. *Cell Death Dis*. **9**(8):820. doi: 10.1038/s41419-018-0886-1.
30. Oliveira, A.N. et al. (2018). Effect of Tim23 knockdown in vivo on mitochondrial protein import and retrograde signaling to the UPRmt in muscle. *Am J Physiol Cell Physiol*. **315**(4):C516-C526. doi: 10.1152/ajpcell.00275.2017.

## **Warranty**

These products are warranted to perform as described in their labeling and in Cell Biolabs literature when used in accordance with their instructions. THERE ARE NO WARRANTIES THAT EXTEND BEYOND THIS EXPRESSED WARRANTY AND CELL BIOLABS DISCLAIMS ANY IMPLIED WARRANTY OF MERCHANTABILITY OR WARRANTY OF FITNESS FOR PARTICULAR PURPOSE. CELL BIOLABS' sole obligation and purchaser's exclusive remedy for breach of this warranty shall be, at the option of CELL BIOLABS, to repair or replace the products. In no event shall CELL BIOLABS be liable for any proximate, incidental or consequential damages in connection with the products.